AIAA Guidance, Navigation, and Control Conference
13 - 16 August 2012, Minneapolis, Minnesota

AIAA 2012-4897

Robust Aeroservoelastic Control Utilizing Physics-Based Aerodynamic Sensing

Gary J. Balas *, Claudia Moreno †, and Peter J. Seiler ‡
Department of Aerospace Engineering and Mechanics
University of Minnesota
Minneapolis, Minnesota

The paper describes the design of aeroservoelastic controllers using H_∞ and LPV control design techniques for a Body Freedom Flutter aircraft. The controllers are compared in the frequency and time domain The LPV controller does not achieve the level of performance of the individual H_∞ controllers, though the performance achieves the desired objectives. The similarities and difference between the designs are discussed.

I. Introduction

The need for improved performance and reduced operating costs has led modern aircraft designers to adopt light-weight, high aspect ratio wings. However, the high flexibility and significant deformation in flight exhibited by these aircraft increase the interaction between the rigid body and structural dynamics modes resulting in Body Freedom Flutter. This phenomenon occurs as the aircraft short period mode frequency increases with airspeed and comes close to a wing vibration mode. This lead to poor handling qualities and may even generate dynamics instability. Hence, an integrated active approach to flight control and flutter suppression is required to meet the desired handling quality performance without compromise structural weight and flight envelope.

This paper presents the design of H_{inf} and linear, parameter-varying controller for a Body Freedom Flutter (BFF) vehicle developed by the Air Force Research Laboratory to demonstrate active aeroelastic control technologies. The vehicle is a high aspect ratio flying wing with light weight airfoil. The aircraft configuration with the location of accelerometers and control surfaces for flutter suppression is presented in the Figure 1.

The aeroservoelastic (ASE) model of the BFF vehicle was assembled using MSC/NASTRAN. A Ground Vibration Test was performed to validate the structural model and six critical modes were found. Table 1 lists the mode shapes and frequency values of the structural model.[1–3]

Table 1. Ground Vibration Test Frequencies

Mode shape:	Frequency (rad/s)
Symmetric Wing 1st Bending	35.37
Anti-symmetric Wing 1st Bending	54.98
Symmetric Wing 1st Torsion	123.34
Anti-symmetric Wing 1st Torsion	132.76
Symmetric Wing 2nd Bending	147.28
Anti-symmetric Wing 2nd Bending	185.73

*balas@umn.edu
†moren148@umn.edu
‡seile017@umn.edu

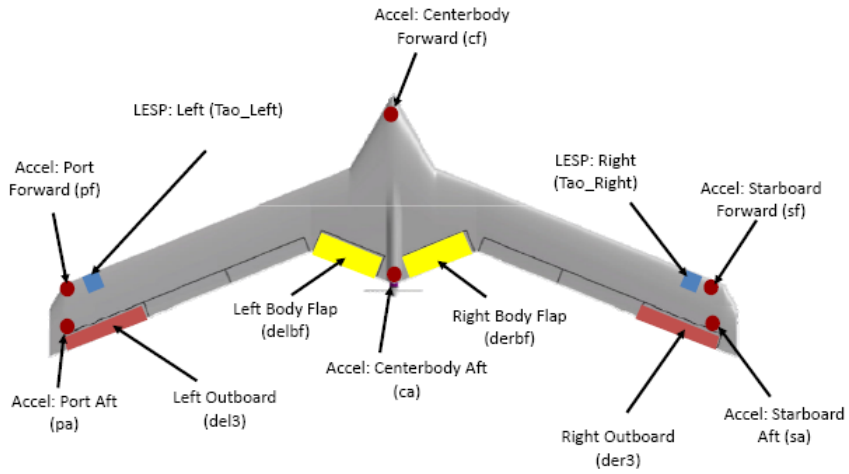

Figure 1. Body Freedom Flutter (BFF) Vehicle. Source: Lockheed Martin Co.

The aerodynamics were modeled using the doublet lattice method. The mass, stiffness and aerodynamics matrices were combined using the P-K method. Finally, the unsteady aerodynamics is approximated with a rational function to create a continuous-time aeroservoelastic state-space model of the airframe with 148 states. The general state-space form of the model is given by Eq. (1)

$$\begin{bmatrix} \dot{x}_p \\ \dot{x}_q \\ \dot{x}_{\omega 1} \\ \dot{x}_{\omega 2} \end{bmatrix} = \begin{bmatrix} 0 & I & 0 & 0 \\ A_{21} & A_{22} & A_{23} & A_{24} \\ 0 & I & \omega_1 I & 0 \\ 0 & I & 0 & \omega_2 I \end{bmatrix} \begin{bmatrix} x_p \\ x_q \\ x_{\omega 1} \\ x_{\omega 2} \end{bmatrix} + \begin{bmatrix} B_1 \\ B_2 \\ 0 \\ 0 \end{bmatrix} u \tag{1}$$

Eq. (1) represents a typical second order equation of motion with augmented state vector due to the rational functions approximation. The state vector consists of modal displacements, x_p, modal velocities, x_q, and two lags states, $x_{\omega 1}$, $x_{\omega 2}$, for the unsteady aerodynamic rational function approximation. Moreover, each set of states is related with 5 rigid modes, 8 flexible modes and 24 secondary discrete degrees-of-freedom listed in Table I.

A set of state space matrices was generated in 2 knot increments from 40 to 90 KEAS (knots equivalent airspeed) with variable Mach at constant altitude of 3000 ft. The frequency and damping of the critical modes for the BFF vehicle are plotted at Fig. 2 as a function of airspeed.

The coupling of the short period with the symmetric wing bending produces BFF at 43 KEAS at 24.3 rad/s. Flutter is also presented when the symmetric wing bending and torsion modes are coupled at an airspeed of 58 KEAS with frequency of 65 rad/s and when the anti-symmetric wing bending and torsion modes comes close in proximity at 61 KEAS and frequency of 69 rad/s. Clearly, the flight envelope of the open-loop vehicle is limited until 42 KEAS before it becomes unstable. Hence, an active control using the control surfaces and structural feedback to stabilize and meet the desired handling qualities of the BFF vehicle is presented.

II. Model Reduction

The inclusion of the structural dynamics and aeroelastic effects result in linear, dynamic models with large number of degrees-of-freedom defined across the flight envelope. It is unrealistic to use these high order and complex models for control design since modern control methods will result in controllers with very high state order. Even more, practical implementation of high order controllers is usually avoided since numerical errors may increase and the resulting system may present undesired behavior. Hence, a reduced-order linear model of the flexible aircraft is necessary to design linear parameter-varying controllers.

Table 2. Model States Names

1	Rigid body lateral	21	Asym body flap rotation
2	Rigid body plunge	22	Right body flap act end 1
3	Rigid body roll	23	Right body flap act end 2
4	Rigid body pitch	24	Left body flap act end 1
5	Rigid body yaw	25	Left body flap act end 2
6	Sym wing 1st bending	26	Right inbd flap act end 1
7	ASym wing 1st bending	27	Right inbd flap act end 2
8	Sym wing 1st torsion	28	Left inbd flap act end 1
9	ASym wing 1st torsion	29	Left inbd flap act end 2
10	Sym wing 2nd bending	30	Right mid flap act end 1
11	Sym wing fore and aft	31	Right mid flap act end 2
12	ASym wing 2nd bending	32	Left mid flap act end 1
13	Right body flap rotation	33	Left mid flap act end 2
14	Left body flap rotation	34	Right outbd flap act end 1
15	Right inboard flap rotation	35	Right outbd flap act end 2
16	Left inboard flap rotation	36	Left outbd flap act end 1
17	Right midboard flap rotation	37	Left outbd flap act end 2
18	Left midboard flap rotation		
19	Right midboard flap rotation		
20	Left midboard flap rotation		

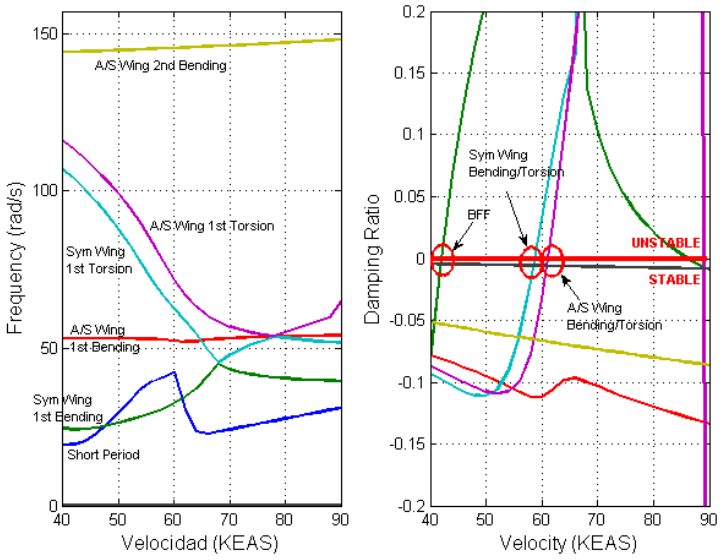

Figure 2. Open loop flutter results

The linear, coupled state-space models of the vehicle generated across the flight envelope are function of the dynamic pressure and Mach. These models are written as

$$\begin{bmatrix} \dot{x}(t) \\ y(t) \end{bmatrix} = \begin{bmatrix} A(\rho) & B(\rho) \\ C(\rho) & D(\rho) \end{bmatrix} \begin{bmatrix} x(t) \\ u(t) \end{bmatrix} \tag{2}$$

$A(\rho)$ is the state matrix, $B(\rho)$ is the input matrix, $C(\rho)$ is the output state matrix, $D(\rho)$ is the input feed through matrix and ρ is a vector that is function of time. These model is a linear parameter-varying (LPV) system. Initially, traditional truncation and modal residualisation techniques are applied to the 147 BFF vehicle model to reduce the state order of the model. The resulting model retain the same 43 states are obtained across the flight envelope. LPV model reduction techniques are used to further reduce the 43 state LPV model to 26 states.[4]

The 26 state LPV BFF vehicle model, which varies as a function of air speed, is used for control design. Initially, at each flight condition a H_∞ controller is synthesized. The H_∞ control designs provide a lower bound on what is achievable by a LPV controller. In addition, the H_∞ problem formulation is used in the design of the LPV controller.

III. H_∞ Control Design

The control design objective is to stabilize the body freedom flutter modes across the flight envelope and increase attenuation of flexible body modes up to 60 rad/s. The controller is synthesized based on the 26 states reduced BFF model. The inputs to the airframe are the four control actuators corresponding to the right and left body flaps and outboard flaps. The output measurements are the three vehicle rates, roll, pitch and yaw rates, and the six accelerometers at the wings and body of the vehicle.

Actuators have a bandwidth of 0-20 Hz and are represented as second-order transfer functions, ${\omega_n}^2/(s^2+2\zeta\omega_n s+{\omega_n}^2)$, where $\omega_n = 125.66$ and $\zeta = 0.65$. Sensors are filtered through a third-order filter, $(\beta/(s+\beta)) \times ({\omega_s}^2/(s^2+2\zeta_s\omega_s s+{\omega_s}^2))$, where $\beta = 360$, $\omega_s = 474$ and $\zeta_s = 0.376$. The reduced order model including actuators and sensors dynamics results in a 61 state-space model. A 61 state design model will challenge the LPV synthesis algorithms. Hence,

The actuators are treated as unity in the control design to reduce the order of the control design model. This is a valid assumption as the actuators are of sufficiently high bandwidth such that they do not limit the performance of the control bandwidth. A first order filter, $\alpha/(s+\alpha)$ with $\alpha = 200$ is used to approximate the phase delay associated with the third order sensors dynamics. Hence, the reduced model for synthesis is a 33 state-space model. Figures 3 and 4 shows the 33 and 182-states models at 40 and 62 KEAS from selected actuators to accelerometers in the wing and body of the vehicle. It is obvious from the Bode plots of these transfer functions the BFF dynamics change significantly across the flight envelope.

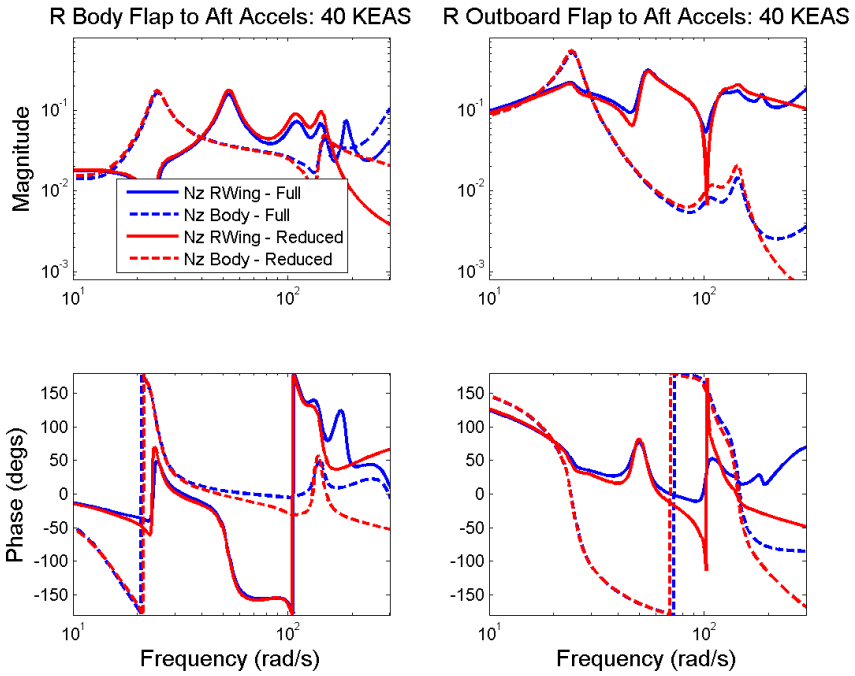

Figure 3. Full and reduced order models with first order filter from body and outboard flap to right wing (RW) and body aft (BA) accelerometers at 40 KEAS

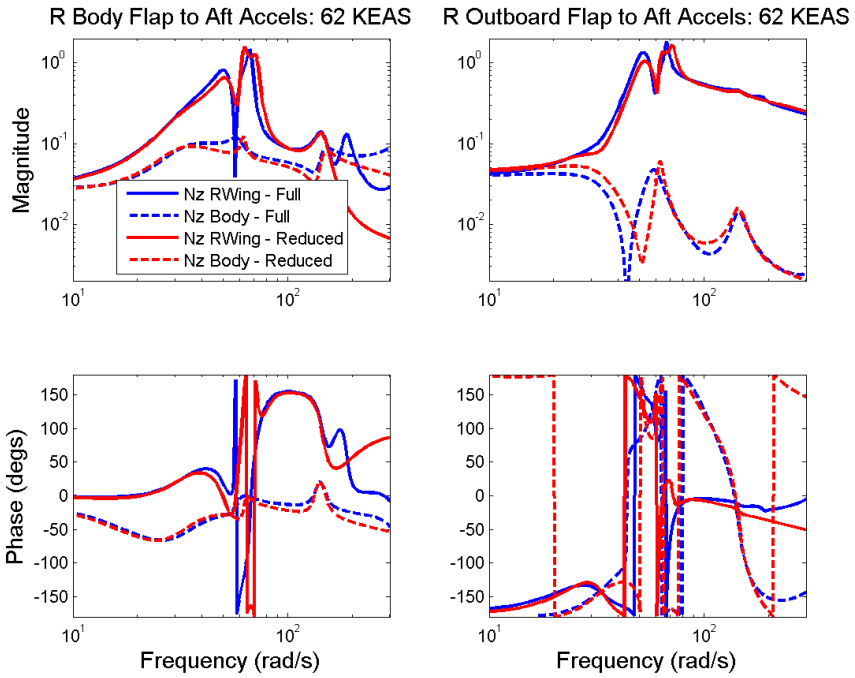

Figure 4. Full and reduced order models with first order filter from body and outboard flap to right wing (RW) and body aft (BA) accelerometers at 62 KEAS

The control objective for the BFF vehicle is to attenuate structural vibration at the wings due to input disturbances at the control surfaces. The controller use the six accelerometers at the wings and body and the pitch rate for feedback. The actuators used for control are the left and right body flaps and outboard flaps, see Figure 1. Controllers are initially synthesized from 40 to 62 KEAS. Upon successfully stabilizing the vehicle using feedback as it transitions from stable linear model at 40 KEAS to an unstable vehicle with 3 unstable modes at 62 KEAS, the controller range will be expanded to the entire flight envelope.

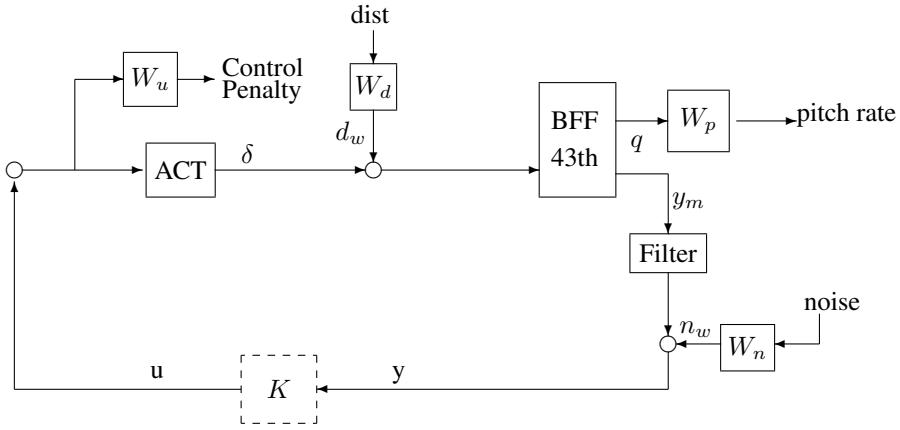

Figure 5. System interconnection for controller synthesis

A block diagram of the H_∞ problem formulation is shown in Fig. 5. The control design model, BFF, consist of the 26 state reduced model of the airframe. The control problem is formulated as a standard, simplified mixed sensitivity. It focuses on stability and flexible mode attenuation of the aeroservoelastic vehicle at each flight condition. One would need to augment the aeroservoelastic control systems with a traditional outer-loop pitch, roll, yaw rigid body flight control system. Future work looks to integrate the rigid body and aeroservoelastic flight control algorithms for flight

control, gust load alleviation and flutter suppression.

The overall objective is to design a LPV controller which schedules the flight controller as a function of airspeed to achieve the desired performance and robustness objective across the flight regime. This section focuses on the synthesis of point design H_∞ controllers.

The performance weighting functions are scaled such that when the weighted H_∞ norm between the actuator disturbances and output modes is below 1, the performance is achieved. A constant weight, W_d equal to 0.5, is used to model the impulse disturbance to each actuator. W_p weights on the pitch rate output and is set to 0.1. The weighting on the actuator command, W_u, is 0.3. The feedback accelerometers are filtered with a first order filter, $200/(s+200)$ to account for the phase lag and roll-off of the filter. The noise weight on the filtered accelerometers is modeled as 0.01 and the pitch rate feedback signal noise weight is 0.10.

A set of controllers across the flight envelope are designed using the interconnection in Fig. 5. The controller receives seven measurement and generates four actuator commands. The controller gains from pitch rate and the right wing aft accelerometer to the right wing body and outboard flaps are shown in Figure 6. Note that the controller response changes significantly as a function of airspeed. Singular values of the frequency response for the closed-loop system at 40 and 62 KEAS are plotted in Fig. 7. The point design H_∞ controllers are able to achieve similar levels of performance at the 40 and 62 KEAS flight conditions.

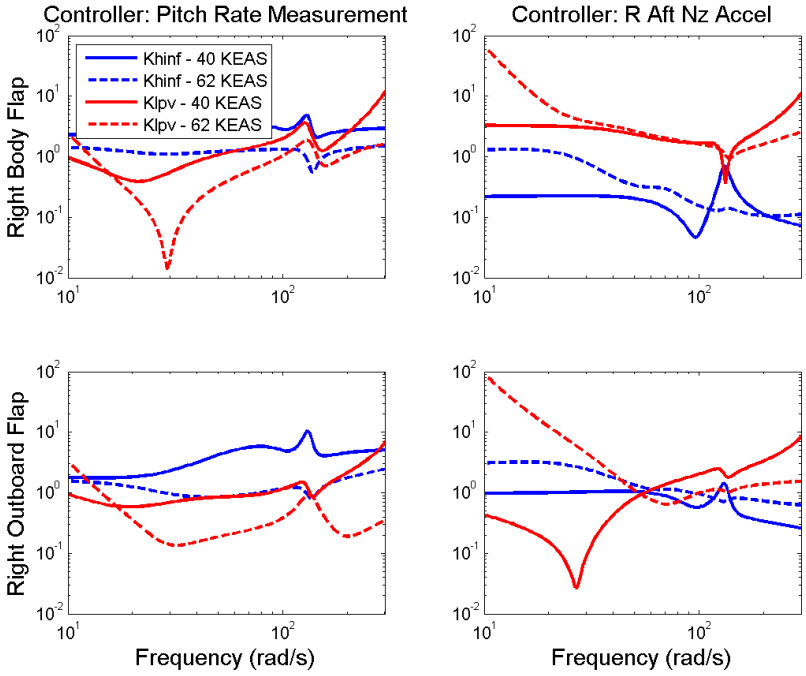

Figure 6. H_∞ and LPV controller gains at 40 and 62 KEAS airspeed

Each controller is simulated with the corresponding BFF aircraft model and the interconnection in Fig. 8. Time responses for the same velocities are plotted in Fig. 9. Note that the H_∞ controllers at 40 and 62 KEAS stabilize the aircraft and provide additional attenuation to the flexible body modes of the vehicle.

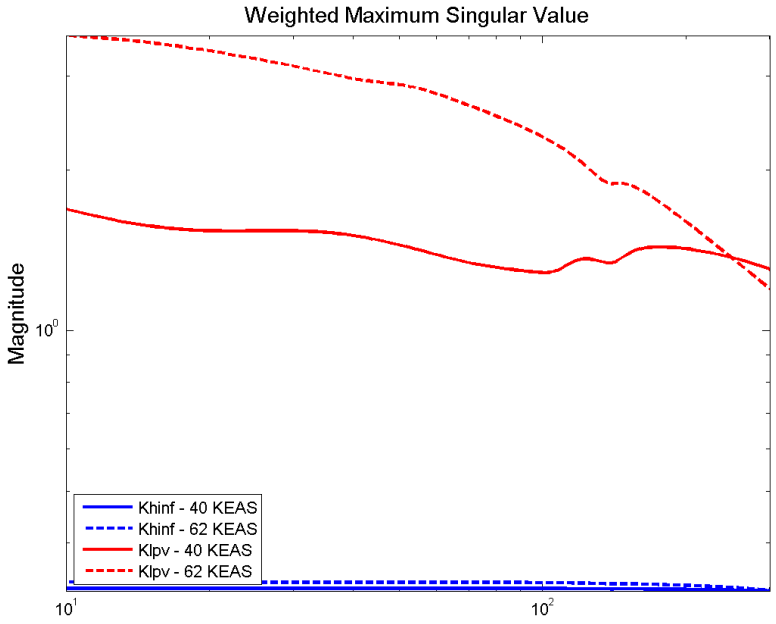

Figure 7. H_∞ **and LPV weighted closed-loop singular values at 40 and 62 KEAS airspeed**

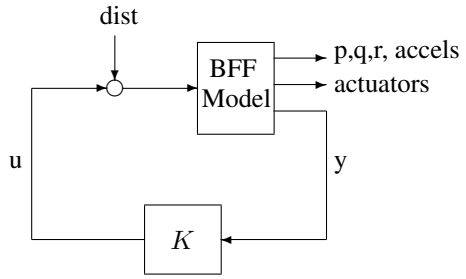

Figure 8. Interconnection for closed-loop system simulation

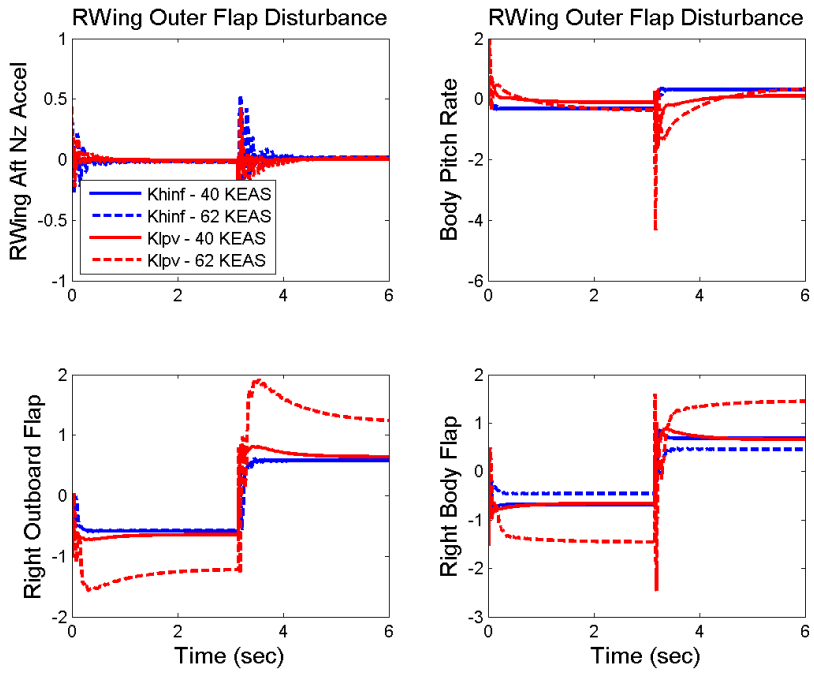

Figure 9. H_∞ **and LPV time simulations due to a right wing outer flap square wave disturbance at 40 and 62 KEAS airspeed**

IV. Linear Parameter Varying Systems

In modeling a large, complex physical system with a non-linear, finite-dimensional state-space model, one chooses a collection of state variables for which the underlying dynamic evolution is understood, giving rise to the state equations. If this is a modestly sized state-space description, then large parts of the dynamic evolution of the "true" states are not represented. The state-space description will involve other variables, called *exogenous*, which have the certain properties:

- the dynamic evolutionary rules for the exogenous variables behavior is not understood, or is too complicated to be modeled;
- the values of the exogenous variables affect (in a known manner) the evolutionary rules which govern the dynamics of the state variables;
- the values of the exogenous variables change with time, but are measurable in real-time using sensors

If a large number of sensors are used, some sensors are measuring outputs in the system theoretic sense (ie., known, explicit nonlinear functions of the modeled states and time), while other sensors are accurate estimates of the exogenous variables. Hence, the model will be a time-varying, nonlinear system, with the future time-variation *unknown*, but measured by the sensors in real-time. In this case, if $\rho(t)$ denotes the exogenous variable vector, and $x(t)$ denotes the modeled state, then the state equations for the system have the form

$$\begin{array}{rcl} \dot{x}(t) & = & f(x(t), \rho(t), u(t)) \\ y(t) & = & h(x(t), \rho(t), u(t)) \end{array} \tag{3}$$

where $u(t)$ is the input (control). The entire trajectory ρ is not known, though the value of $\rho(t)$ is known at time t, and hence may be used in any control strategy.

If in equation (3) f and h are linear in the pair $[x, u]$, then the system appears as

$$\begin{array}{rcl} \dot{x}(t) & = & A(\rho(t))x(t) + B(\rho(t))u(t) \\ y(t) & = & C(\rho(t))x(t) + D(\rho(t))u(t) \end{array} \tag{4}$$

and is called *linear parameter-varying* (LPV).

The scheduled variable or vector, $\rho(t)$, for LPV systems is assumed to be an exogenous signal. If the scheduled variable contains or is entirely composed of system states then the system is called a *quasi-LPV* system. Treating a quasi-LPV system as an LPV system ignores the fact that the value of $\rho(t)$ depends on the system states x, instead $\rho \in \mathbf{R}^{s+m}$ is treated as an independent exogenous parameter and resulting in the LPV model in equation (4). Note that this is the conservative step, as it introduces additional behavior that the real system cannot actually exhibit. For aircraft, it is often the case that a gain-scheduled controller would schedule as a function of a system state, e.g. velocity and altitude. Hence, current gain-scheduled flight controllers would be a quasi-LPV system.

A. Controlling Parameter-dependent Systems

We begin with a brief introduction to gain-scheduling based on linear parameter-varying (LPV) plant representations. The system in equation (4) is said to be quadratically stable if there exists a matrix $X = X^T > 0$ such that

$$A^T(\rho)X + XA(\rho) < 0,$$

for all $\rho \in \mathcal{P}$. It is well known that if the system (4) is quadratically stable then it is exponentially stable for any parameter trajectory $\rho(\cdot) \in \mathcal{F}_{\mathcal{P}}$. The induced $\mathcal{L}_2$ norm of a LPV system $G_{\mathcal{F}_{\mathcal{P}}}$, with zero initial conditions, is defined as

$$\|G_{\mathcal{F}_{\mathcal{P}}}\| \doteq \sup_{\rho \in \mathcal{F}_{\mathcal{P}}} \sup_{\substack{\|d\|_2 \neq 0, \\ d \in \mathcal{L}_2}} \frac{\|e\|_2}{\|d\|_2}. \tag{5}$$

It is well known that if $G_{\mathcal{F}_{\mathcal{P}}}$ is quadratically stable then this quantity is finite.

From the point of view of control design we assume that the plant has the partitioned LPV representation,

$$\begin{bmatrix} \dot{x}(t) \\ e(t) \\ y(t) \end{bmatrix} = \begin{bmatrix} A(\rho) & B_1(\rho) & B_2(\rho) \\ C_1(\rho) & D_{11}(\rho) & D_{12}(\rho) \\ C_2(\rho) & D_{21}(\rho) & D_{22}(\rho) \end{bmatrix} \begin{bmatrix} x(t) \\ d(t) \\ u(t) \end{bmatrix}, \tag{6}$$

where $\rho \in \mathcal{F}_{\mathcal{P}}$, $y \in \mathcal{R}^{n_y}$ is the measurement, $u \in \mathcal{R}^{n_u}$ is the control input, $d \in \mathcal{R}^{n_d}$ is the exogenous disturbance, and $e \in \mathcal{R}^{n_e}$ is the error output. It is assumed that the parameter $\rho(\cdot)$ can be measured in real-time, and that the controller is of the form

$$\begin{bmatrix} \dot{x}_K(t) \\ u(t) \end{bmatrix} = \begin{bmatrix} A_K(\rho(t)) & B_K(\rho(t)) \\ C_K(\rho(t)) & D_K(\rho(t)) \end{bmatrix} \begin{bmatrix} x_K(t) \\ y(t) \end{bmatrix}, \tag{7}$$

where $\rho \in \mathcal{F}_{\mathcal{P}}$.

The "quadratic LPV γ-performance problem" is to choose the parameter-varying controller matrices $A_K(\rho)$, $B_K(\rho)$, $C_K(\rho)$, $D_K(\rho)$ such that the resultant closed-loop system is quadratically stable and the induced $\mathcal{L}_2$ norm from d to e is $\leq \gamma$. It is well known that the quadratic LPV γ-performance problem is solvable if there exists an integer $m \geq 0$, a matrix $W \in \mathcal{R}^{(n+m)\times(m+n)}$, $W = W^T > 0$ and continuous bounded matrix functions $(A_K, B_K, C_K, D_K) : \mathcal{R}^s \to (\mathcal{R}^{m\times m}, \mathcal{R}^{m\times n_y}, \mathcal{R}^{n_u\times m}, \mathcal{R}^{n_u\times n_y})$ such that

$$\begin{bmatrix} A_{clp}^T(\rho)W + WA_{clp}^T(\rho) & WB_{clp}(\rho) & \gamma^{-1}C_{clp}^T(\rho) \\ B_{clp}^T(\rho)W & -I_{n_d} & \gamma^{-1}D_{clp}^T(\rho) \\ \gamma^{-1}C_{clp}(\rho) & \gamma^{-1}D_{clp}(\rho) & -I_{n_e} \end{bmatrix} < 0, \tag{8}$$

for all $\rho \in \mathcal{P}$, where the matrices A_{clp}, B_{clp}, C_{clp} and D_{clp} are the closed-loop state-space data.

The main result is that the existence of a controller that solves the quadratic LPV γ-performance problem can be expressed as the feasibility of a set of Affine Matrix Inequalities (AMIs), which can be solved numerically. For more details on LPV synthesis results the reader is referred to.[7–9,11] The parameter ρ is assumed to be available in real time, and hence it is possible to construct an LPV controller whose dynamics adjust according to variations in ρ, and maintain stability and performance along all parameter trajectories. This approach allows gain-scheduled controllers to be treated as a single entity, with the gain-scheduling achieved via the parameter-dependent controller. For more details on inclusion of bounds on the rate-of-variation of the scheduled parameters, the reader is referred to.[12,15,16]

V. LPV Control Design

LPV controllers are synthesized for the BFF vehicle across airspeed based on the control problem formulation shown in Fig. 5. The flight envelope is taken to be between 40 and 66 KEAS in this study. A new linear model of the BFF aircraft is defined at every 2 KEAS. The same weighting functions used for the H_∞ point designs as used for the LPV control problem formulations. The BFF model in Fig. 5 now represents the BFF LPV model from 40 to 66 KEAS, which corresponds to 14 plant models.

Non-rate bounds LPV control design algorithms were initially used to synthesize controllers. The algorithms can back infeasible which indicated that it was not possible to synthesize a LPV controller which allowed airspeed to vary infinitely fast. This result was expected since the stability of the BFF model changes across the flight envelope. A non-rate bounds LPV controller would allow the vehicle model to switch infinitely fast between a stable and unstable plant. Hence, rate-bounded LPV synthesis algorithms were used to design the parameter-varying controllers.[12,15,16] The rate of change of airspeed was limited to ± 0.01 knots/sec which corresponds to velocities of ± 36 knots/hr. This is close to the expected rate of variation of the actual BFF vehicle in flight.

The LPV controller gains from pitch rate and the right wing aft accelerometer to the right wing body and outboard flaps are shown in Figure 6. The LPV controller gains at the 40 and 62 KEAS points are significantly different than the gains of the H_∞ point designs. Similarly, the singular values of the frequency response for the closed-loop system at 40 and 62 KEAS with the LPV controller implemented are plotted in Fig. 7. The point design performance of the LPV controllers are significantly worse that the H_∞ point designs. The reason for this large difference is under investigation.

Time responses of the LPV design at the same velocities as the H_∞ controllers are plotted in Fig. 9. Note that both the LPV and H_∞ controllers at 40 and 62 KEAS stabilize the aircraft and provide additional attenuation to the flexible

body modes of the vehicle. There is a noticeable low frequency gain difference with the LPV and H_∞ controllers implemented. This indicates it was challenging for the LPV rate-bounded controller synthesis algorithm to find a parameter-varying controller which stabilized all the plant models in the set and achieved the desired performance. As was noted in figures 3 and 4, the BFF dynamics change dramatically across the flight envelope. The rate-bounded LPV control design algorithms may require additional parameter basis functions to be included in the design to better capture the characteristics associated wit the variation of the airspeed. This is being investigated.

VI. Summary

The paper presented the results of the control of the BFF vehicle using H_∞ and LPV control design techniques. The performance and robustness of the LPV controller are compared with the individual H_∞ point design controllers. The LPV controller does not achieve the level of performance of the individual H_∞ controllers, though the performance achieves the desired objectives. The benefit of the LPV controllers is that they guarantee the stability and performance of the closed-loop aircraft across the flight envelope.

A. Acknowledgment

This work was funded as part of a NASA STTR contract NNXIICI09P entitled "Robust Aeroservoelastic Control Utilizing Physics-Based Aerodynamic Sensing." Dr. Arun Mangalam of Tao Systems is the Principal Investigator on the contract and Dr. Martin Brenner is the NASA technical monitor.

References

[1]J. Beranek, L. Nicolai, M. Buonanno, E. Burnett, C. Atkinson, B. Holm-Hansen and P. Flick, "Conceptual design of a multi-utility aeroelastic demonstrator," *13th AIAA/ISSMO Multidisciplinary Analysis Optimization Conference*, Fort Worth, TX, 2010.

[2]E. Burnett, C. Atkinson, J. Beranek, B. Sibbitt, B. Holm-Hansen and L. Nicolai, "NDOF Simulation model for flight control development with flight test correlation," *AIAA Modeling and Simulation Technologies Conference*, Toronto, Canada, 2010.

[3]B. Holm-Hansen, C. Atkinson, J. Beranek, E.L. Burnett, L. Nicolai and H. Youssef, "Envelope expansion of a flexible flying wing by active flutter suppression, *AUVSI's Unmanned Systems North America*, Denver, CO, 2010.

[4]C.P. Moreno, P. Seiler, and G.J. Balas, " Linear, Parameter Varying Model REduction for Aeroservoelastic Systems," *AIAA Flight Mechanics Conference*, Minneapolis, MN USA, 2012.

[5]Gary Balas, Ian Fialho, Andy Packard, Joe Renfrow and Chris Mullaney, "On the design of LPV controllers for the F-14 aircraft lateral-directional axis during powered approach," *1997 American Control Conference*, Albuquerque, pp. 123-127, June 1997.

[6]Gary Balas, Ian Fialho, Andy Packard, Joe Renfrow and Chris Mullaney, "Linear fractional transformation control for the F-14 aircraft lateral-directional axis during powered approach," *1997 American Control Conference*, Albuquerque, pp. 128-132, June 1997.

[7]G. Becker, "Quadratic stability and performance of linear, parameter-dependent systems," PhD Thesis, Mechanical Engineering, University of California, Berkeley, December 1993.

[8]Gregory Becker and Andy Packard, "Robust performance of linear, parametrically varying systems using parametrically-dependent linear dynamic feedback," *Systems and Control Letters*, vol. 23, pp. 205-215, September 1994.

[9]G. Becker, A. Packard, D. Philbrick and G. Balas, "Control of parametrically dependent linear systems: a single quadratic Lyapunov approach," *1993 American Control Conference*, pp. 2795-2799, June 1993.

[10]C.M. Belcastro and B.C. Chang, "LFT Formulation for Multivariate Polynominal Problems," *1998 American Control Conference*, Philadelphia, PA, June, 1998, pp. 1002-1007.

[11]A. Packard and G. Becker, "Quadratic stabilization of parametrically dependent linear systems using parametrically dependent linear feedback," DSC-Vol. 43 *Advances in Robust and Nonlinear Control Systems*, pp. 29-36, ASME Winter Annual Meeting, November 1992.

[12]Fen Wu, Andy Packard and Gary Balas, "LPV control design for pitch-axis missile autopilots," *1995 Conference on Decision and Control*, New Orleans, pp. 188-193, Dec. 1995.

[13]Fen Wu and Andy Packard, "Optimal LQG performance of linear, uncertain systems using state-feedback," *1995 American Control Conference*, Seattle, pp. 4435-4439, June 1995.

[14]Fen Wu and Andy Packard, "LQG control design for LPV systems," *1995 American Control Conference*, Seattle, pp. 4440-4444, June 1995.

[15]F. Wu, "Control of linear paramneter varying systems," PhD dissertation, Department of Mechanical Engineering, University of California, Berkeley, 1995. Available via anonymous FTP at
`jagger.me.berkeley.edu`.

[16]Fen Wu, Xin Hua Yang, Andy Packard and Greg Becker, "Induced $\mathcal{L}_2$ norm control for LPV systems with bounded parameter variation rates," *International Journal of Nonlinear and Robust Control*, vol. 6, pp. 983-998, 1996.